

Anomalous Cis Isomer Orientation in a Liquid Crystalline Azo Polymer on Irradiation with Linearly-Polarized Light

Dennis K. Hore[†] and Almeria L. Natansohn

Department of Chemistry, Queen's University, Kingston, ON K7L 3N6, Canada

Paul L. Rochon*

Department of Physics, Royal Military College, P.O. Box 17000, Station Forces, Kingston, ON K7L 7B4, Canada

Received: June 12, 2002; In Final Form: December 12, 2002

An azo-containing liquid crystalline polymer was irradiated with linearly polarized blue Ar⁺ light and the resulting linear birefringence and dichroism were monitored. In its amorphous phase, results obtained are typical for azo polymers of similar structure, with the optical constants largest along the direction perpendicular to the laser polarization. In its nematic phase, surprising results are obtained, including two changes in the sign of the dichroism measured at 632.8 nm and, at one point, a quadrupolar transmission profile. Dichroic visible spectra show evidence for two bands of opposite sign in the region of the $n\pi^*$ transition, which are attributed to the trans and cis isomers. In addition to the conventional photoreorientation of azo groups along an axis perpendicular to the polarization direction of the pump, we propose that, under some conditions, a tendency toward parallel alignment occurs as a result of the optical Fréedericksz transition.

1. Introduction

The spectroscopy of azobenzene and its derivatives has been widely studied by both experimental and theoretical means. Much of this effort is focused toward understanding the photochemical and/or thermal isomerization of these compounds. The experimental data have been reviewed by Rau,¹ the theoretical work has been discussed by Monti et al.² and more recently by Ishikawa et al.³ In the near-UV the two lowest-lying transitions $^1(n\pi^*)$ and $^1(\pi\pi^*)$ are observed for both trans and cis isomers, although it is difficult to separate the $^1(n\pi^*)$ transitions for the two isomers on account of their proximity.^{4–6} For the trans isomer the $^1(n\pi^*)$ transition is symmetry-forbidden but has considerable intensity, likely borrowed from a nearby $\pi\pi^*$ state.⁷ This transition is also more intense in substituted azobenzenes.¹ There are also four additional low-lying triplet states, $^3(n\pi^*)$ and $^3(\pi\pi^*)$ for each isomer, but these have never been directly observed. For the present study, the important characteristic of these excited states is that they all have the irreducible representation B for the cis isomer with C_2 symmetry, or B_g/B_u in the case of the trans isomer with C_{2h} symmetry.² As a consequence, the transition dipole moments are all parallel to the N=N bond axis of the chromophore.⁸

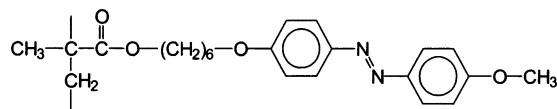
The reorientation of azobenzene-containing materials by means of successive trans–cis–trans isomerizations in an optical field has, by now, been well-studied; the most recent review is given by Delaire and Nakatani.⁹ Changes in the orientation of the molecules occur as a result of the changes in shape accompanying the photoisomerization. When the chromophores happen to fall into an orientation where all their transition dipole moments are perpendicular to the polarization axis of the pump, absorp-

tion, and therefore the accompanying isomerization, is no longer possible and so those molecules become trapped. The phenomenon is most interesting in materials with a rigid or restrictive matrix such as polymers because there exists the possibility of stable reorientation following irradiation. This applies to amorphous materials as well as liquid crystals.^{10,11}

In a liquid crystalline material, however, there are additional possibilities for reorienting molecules. The mechanisms and the ease with which they occur depend on the specific phase of the material. Among the liquid crystalline phases, the nematic phase possesses orientational order only and lacks the positional order found in higher-ordered phases such as smectics. There have been many studies of liquid crystals either doped or functionalized with azo chromophores; reviews are given in refs 12 and 13. The most typical situation is one where reorientation of the azo groups promotes reorientation of the liquid crystal director. Another method of reorienting nematic liquid crystals is by the application of an electric field; the molecules twist so that the director is now aligned parallel to the field. This is an example of the Kerr effect where a torque develops between the induced dipole and electric field; the molecules twist to minimize the torque they experience. In the liquid crystal literature, such reorientation is referred to as the Fréedericksz transition.¹⁴ If the external field is an optical field, then the phenomenon is further qualified as the optical Fréedericksz transition (OFT).^{15–17} Photoisomerization of azo groups doped in a nematic host has been found to greatly reduce the OFT threshold by two mechanisms. First, a high concentration of cis isomers promotes the director to align with the cis long axis, which may be oriented at a considerable angle to that of the former trans.¹⁸ Second, there is a large dye-induced torque that acts on the host in addition to the direct optical torque¹⁹ from the external field. Further, in the case of azo dyes, the induced torque from cis and trans isomers may differ substantially so the OFT dynamics become sensitive to the cis fraction.²⁰ A detailed microscopic

* To whom correspondence should be addressed. E-mail: rochonp@rmc.ca. Phone: 613-541-6000 ext 6451. Fax: 613-541-6040.

[†] Present address: Department of Chemistry, University of Oregon, Eugene, OR 97403.



G 75°C *S_A* 95°C *N* 135°C *I*

Figure 1. Molecular structure and phase sequence of the liquid-crystalline azo polymer pMAB6.

mechanism for this has been proposed by Jánosy in ref 21. Considering all of these effects, the OFT threshold has been shown to be reduced by 2–4 orders of magnitude^{18,21} from typical values of 100 W/cm² required for transparent materials.^{15,22} The material described here, named pMAB6, is an azo-containing liquid crystalline polymer with a room-temperature nematic phase following annealing, and so meets the criteria for both OFT and trans–cis photoreorientation processes. This paper illustrates the competition between alignment due to the OFT and alignment due to azo isomerization.

The film preparation technique and the experimental conditions of the samples will be described first. Next, some details of the Stokes polarimetry experiment, which is used to obtain the order parameters, is given, along with the data obtained using the apparatus while the sample is irradiated. The results of dichroic microscopy and spectral studies are presented next, and are discussed along with the polarimetry results. Finally, two coexisting mechanisms for chromophore reorientation are proposed, which are consistent with the experimental data.

2. Material and Sample Preparation

The polymer used in this study, poly[6-[(4-(methoxyphenyl)-diazanyl)phenyl]oxy]hexyl methacrylate (pMAB6), was prepared for us in a manner similar to that described in refs 23 and 24; its structure and phase sequence are shown in Figure 1. Our sample has a number-average molecular weight of 27 000 and a polydispersity index of 2.1. Glass microscope slides were cleaned with a dilute soap/water solution, rinsed with ethanol and distilled water, and then dried in an oven. Care was taken not to rub the glass slides at any point in the cleaning, as this has been found to influence the liquid crystal alignment. Films were spin-cast from 10–17% (by weight) solutions of the polymer in tetrahydrofuran onto these glass substrates at a speed of 750 rpm. Thickness measurements were obtained using a Sloan Dektak IIA profilometer. Freshly prepared films were transparent and appeared amorphous (dark) under crossed polarizers. The fresh film irradiated in this study had a thickness of 2.8 μm . A second film (thickness 3.5 μm) was annealed by heating to 140 °C (in the isotropic phase), then cooling to room temperature over a period of 10–12 h. After annealing, the film appeared transparent on visual inspection but was now bright through crossed polarizers. Polarized microscopy revealed a typical nematic Schlieren texture, shown in Figure 2. A film was sent for X-ray diffraction measurement before and after annealing and these data are shown in Figure 3. In the liquid crystalline state, the nematic phase is characterized by the absence of a Bragg peak at small angles, as would be observed for a smectic. Some liquid crystalline phases take a long time for their characteristic texture to develop, but these films were monitored over several weeks and the same observations were made. All experiments were performed at room temperature.

3. Polarimetry Study

Orientation was studied using a homemade single-wavelength single-detector Stokes polarimeter²⁵ with a 632.8 nm HeNe laser

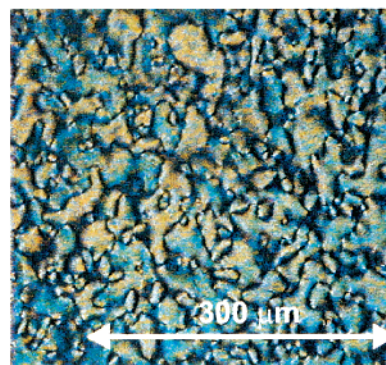


Figure 2. Schlieren texture observed under a polarized microscope for an annealed 4700 nm film of pMAB6 at room temperature.

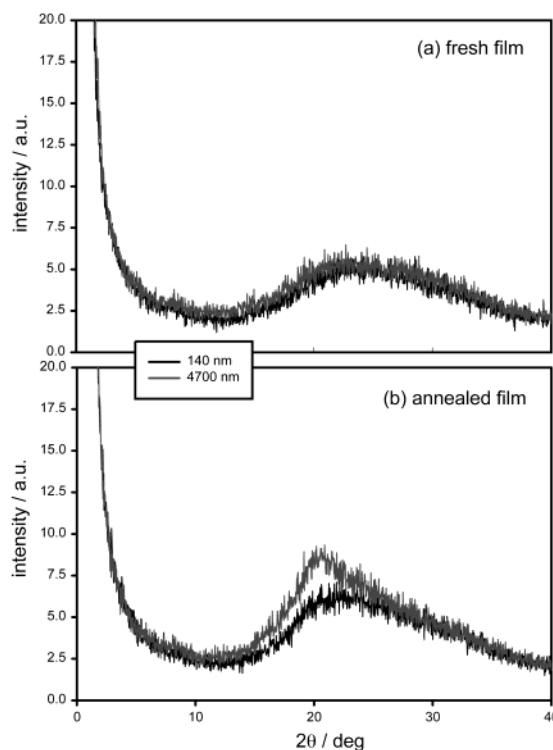


Figure 3. X-ray diffraction for 140 nm and 4700 nm films of pMAB6 (a) before and (b) after annealing at 140 °C for 1 h and then cooling slowly to room temperature.

as a probe. The probe was expanded to a diameter of ca. 5 mm, resulting in an intensity of 5×10^{-2} mW/cm², so that a larger orientational average could be performed. We measured the Stokes parameters (S_0 , S_1 , S_2 , and S_3) of the transmitted light as a function of the azimuth of the linearly-polarized probe for various exposures to the Ar⁺ laser, thereby obtaining complete information on the change in polarization caused by the sample. To interpret the results, we proposed a uniaxial chromophore distribution from which the birefringence, dichroism, and orientation of the optical axis are determined using a model of the polarization transfer. For this, we constructed a polarization transfer operator T , which acts as the sample in altering the polarization as described by the complex electric field

$$E_{\text{out}} = TE_{\text{in}} \quad (1)$$

The details of the model, which include consideration of thin-film interference and anisotropic Fresnel coefficients, are given

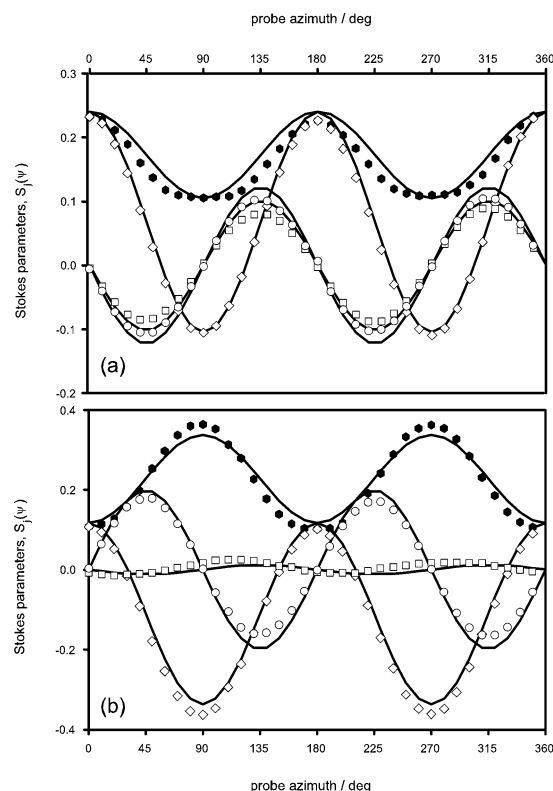


Figure 4. Sample polarimetry data showing the Stokes parameters S_i measured as a function of the probe beam azimuth ψ with (●) S_0 , (◇) S_1 , (□) S_2 , and (○) S_3 . Curves are drawn from the fitting results, showing (a) 16 min exposure with $\Delta n = -0.134$ and $\Delta\alpha = +0.104 \mu\text{m}^{-1}$ and (b) 60 min exposure with $\Delta n = -0.0651$ and $\Delta\alpha = -0.123 \mu\text{m}^{-1}$.

in our previous publication.²⁵ We arrive at the result

$$T = R(-\theta) \begin{bmatrix} t_{\text{slow}} & 0 \\ 0 & t_{\text{fast}} \end{bmatrix} R(\theta) \quad (2)$$

where R is the rotation operator that transforms the coordinate system from the laboratory xy frame through an angle θ to that of the sample's optical axes. The transmission coefficients for the electric field are

$$t_{\text{slow}} = \frac{2n_{\text{air}}}{(n_{\text{air}} + n_{\text{glass}}) \cos(k_0 n_{\text{slow}} d) - i \left(\frac{n_{\text{air}} n_{\text{glass}}}{n_{\text{slow}}} + n_{\text{slow}} \right) \sin(k_0 n_{\text{slow}} d)} \quad (3)$$

with an analogous expression for t_{fast} , where $k_0 = 2\pi/\lambda_0$ and d is the film thickness. The polarization was then determined by expressing E_{out} in terms of the Stokes parameters using

$$\begin{aligned} S_0 &= E_x E_x^* + E_y E_y^* \\ S_1 &= E_x E_x^* - E_y E_y^* \\ S_2 &= E_x E_y^* + E_y E_x^* \\ S_3 &= i(E_x E_y^* - E_y E_x^*) \end{aligned} \quad (4)$$

The films were irradiated with an Ar^+ laser focused to a diameter of 7 mm to achieve an intensity of 90 mW/cm^2 . Each exposure was followed by a 1 min relaxation period before the sample was subjected to the red probe beam, whose transmitted

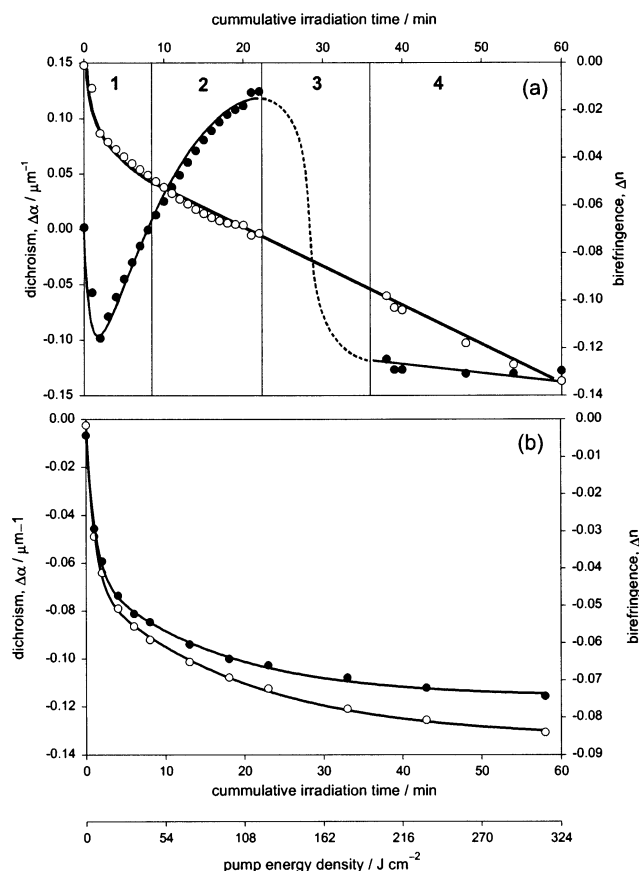


Figure 5. Dichroism (●) and birefringence (○) obtained from fitting a model of the polarization transfer to the experimentally determined Stokes parameters at $\lambda = 632.8 \text{ nm}$. For the annealed film (a) the birefringence decreases monotonically and the behavior of the dichroism is categorized into four distinct regions. The birefringence and dichroism for the fresh film (b) both show a continuous increase in the negative direction.

polarization was determined. Sample data is shown in Figure 4 for cumulative exposures of (a) 16 min and (b) 60 min. A least-squares fitting of the above model to these data using an exhaustive search algorithm (described in ref 25) resulted in the determination of the dichroism, birefringence, and orientation of the optical axis. These results are also shown in Figure 4.

Results of dichroism and birefringence determination for the entire range of exposures are shown in Figure 5. In keeping with the sign conventions used in the model, negative values of the dichroism and birefringence correspond to $\theta = 0^\circ$. In the cases where $\theta = 90^\circ$, the dichroism and birefringence would be represented with positive values. For the annealed film (Figure 5a) the birefringence shows a monotonic increase in magnitude from zero (before irradiation) to nearly -0.14 after 1 h of exposure. The dichroism, on the other hand, starts off tending in the negative direction, then turns around, and approaches zero again (region 1). This tendency continues as the dichroism now takes on positive values (region 2). For a certain range of exposures (region 3) a strange quadrupolar transmission profile was observed (see Figure 6) and it was not possible to fit the data to a model of uniaxial orientation to obtain the birefringence or dichroism. At long exposures, however, a uniaxial distribution was again observed (region 4) and the dichroism was found to be negative. Figure 6 shows the transmission profiles obtained in each of these regions as the azimuth of the linearly-polarized probe is rotated through 360° . For the sample that was not annealed prior to irradiation, and therefore not in a liquid crystalline state, the birefringence

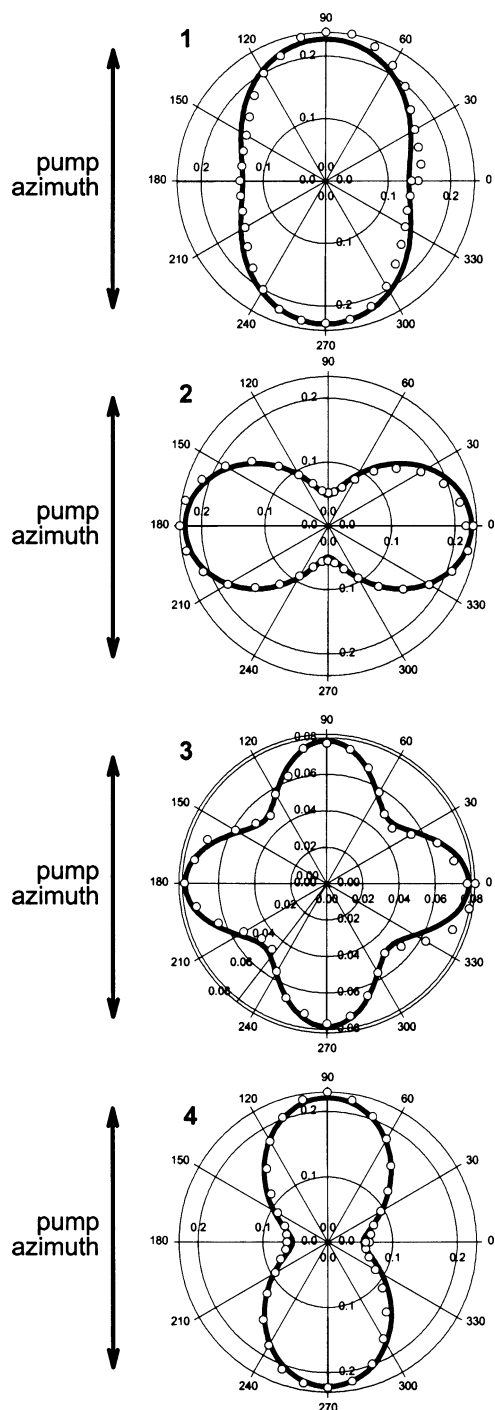


Figure 6. Transmission profiles obtained for exposures characteristic of regions 1–4 of Figure 5.

and dichroism both tend toward increasingly negative values (Figure 5b), as is typically the case for azo polymers exposed to a linearly-polarized pump with vertical azimuth.^{9,26,27}

4. Dichroic Microscopy Study

A microscopy study was made of the quadrupolar transmission profile obtained for the annealed film during intermediate exposures (region 3, Figures 5 and 6). Here a single polarizer, whose azimuth could be rotated, was placed between the microscope lamp and the sample. The image obtained with such a configuration is therefore a two-dimensional map of the dichroism. Because the transmission function of any polarizer has a square cosine intensity distribution, a profile with four

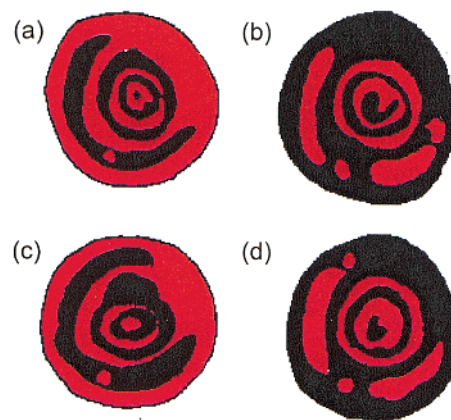


Figure 7. Computer-enhanced-contrast dichroic microscope images obtained for an irradiation time corresponding to an exposure in region 3 of Figure 5. The polarizer angle is (a) 0°, (b) 90°, (c) 180°, and (d) 270° measured counterclockwise from the positive *x*-axis.

TABLE 1: Determination of the Relative Areas of Opposite Contrast in Figure 7. Angles Are Measured Counterclockwise from the Positive *x*-Axis

polarizer angle (deg)	% dark area	% bright area
0	39.2	60.8
90	73.1	26.9
180	50.2	49.8
270	71.7	28.3

maxima cannot be explained on the basis of any static arrangement of chromophores. Indeed, a close examination of the contrast-enhanced optical micrographs in Figure 7 and the corresponding relative areas of high and low contrast presented in Table 1 indicate that the size of the regions are changing during the probing process, both with the red HeNe and under the white light of the optical microscope.

5. Spectral Study

To better understand the origin of the strange positive dichroism observed for the liquid-crystalline (annealed) film, dichroic spectra were obtained from 450 to 650 nm for a few exposures to the vertical (linearly-polarized) pump. These were acquired with a Shimadzu UV-1201 spectrophotometer, modified with a calcite Glan–Thompson prism to acquire dichroic spectra. For these studies, it was necessary to expand the beam to a diameter of 2 cm to irradiate a region large enough to cover the probe beam of the spectrophotometer. Because the time scale of the experiment is increased in proportion to the decrease in intensity, large exposures were achieved using a 200 mW Ar⁺ laser. To best compare the results, we report all data in terms of exposure. (Due to the thickness of the films, the transmittance was too low to scan below 450 nm. The importance of the film thickness will be mentioned later.) Figure 8a shows the spectra obtained for the annealed sample. The dichroism around 470 nm increases monotonically in the negative direction with successive irradiation. For low exposures, a positive band appears around 530 nm. At long irradiation times, this band appears to shift toward shorter wavelengths (nearer to 500 nm) and then drops into the negative region. From a qualitative inspection, it is understood why the birefringence is always negative whereas the dichroism is at times positive. From the Kramers–Kronig relations it is known that the refractive index difference at a single wavelength comes from an integration of the entire dichroic spectrum. Most of the area below the curves is negative and the positive dichroism therefore makes only a small contribution. Dichroic spectra for the freshly prepared film

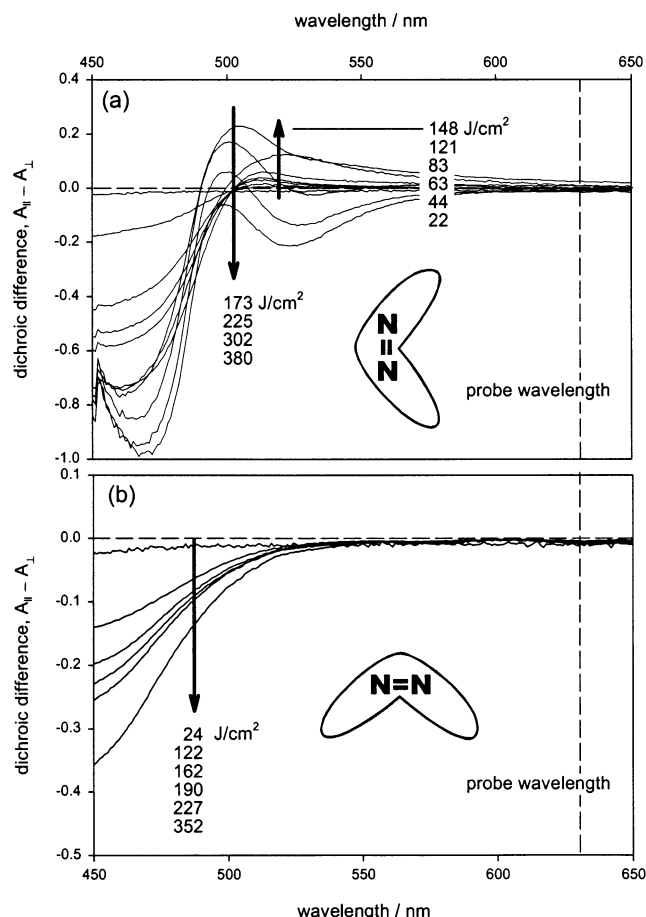


Figure 8. Dichroic difference spectra for successive irradiation times. Arrows indicate the time sequence of the spectral bands. The annealed film is shown in (a) and the fresh film in (b).

are shown in Figure 8b. Here we see only a single negative band, indicating the trans and cis $N=N$ axes are perpendicular to the pump polarization, as is typically observed for azo polymers.

6. Discussion

In the previous section it was mentioned that the dichroic spectra agree with the polarimetry results at 632.8 nm, with the dichroism being twice negative and once positive. The complex shape of these spectra, including the many apparent peaks, may be accounted for with a simple deconvolution to reveal a single negative peak centered at 470 nm and a single positive peak 495 nm. An example of this is shown in Figure 9a; the entire dichroic spectra set may be faithfully recovered using the fitting values for these two peaks, shown in Figure 9b. To interpret these results, we propose that the $n\pi^*$ transitions for the trans and cis isomers, which usually appear as a single convoluted structureless band in the region 440–500 nm, may in this case be seen separately as a result of an unusual orientation of the cis isomers. Because the transition dipole moment is oriented along the $N=N$ bond axis, this would indicate that the trans isomers (470 nm) are oriented with their long axes perpendicular to the polarization direction of the pump, and the cis isomers (495 nm) with their $N=N$ axes parallel to the pump polarization, as shown in the inset of Figure 8a. Figure 10 shows the evolution of the amplitude of the two bands obtained from the deconvolution. The band at 495 nm increased monotonically in the positive direction, as did the band at 470 nm but in the negative direction.

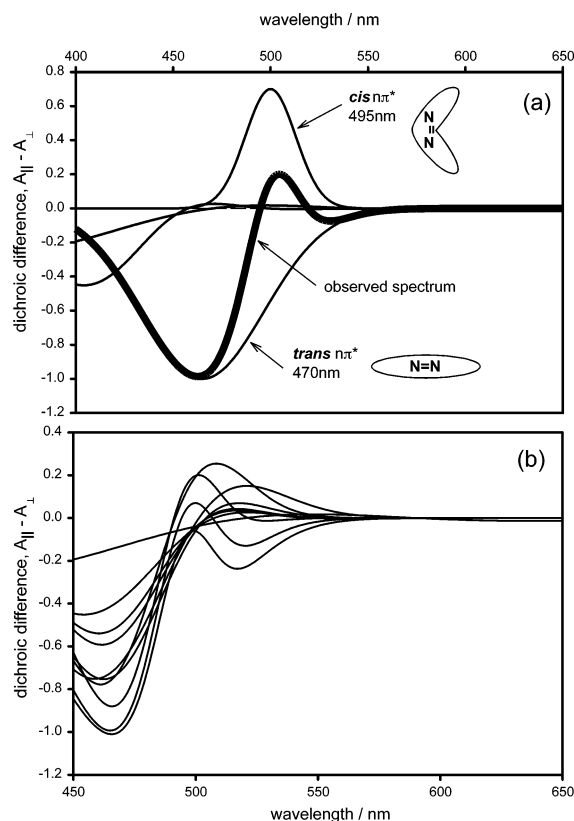


Figure 9. (a) For the liquid-crystalline film, the orientation of the cis isomers allows the $n\pi^*$ transitions for the trans and cis isomers to be separated in the low-energy region of the spectrum. (b) Simulated spectra based on the fitting and convolution of these two bands closely resemble all the experimental dichroic spectra in Figure 8.

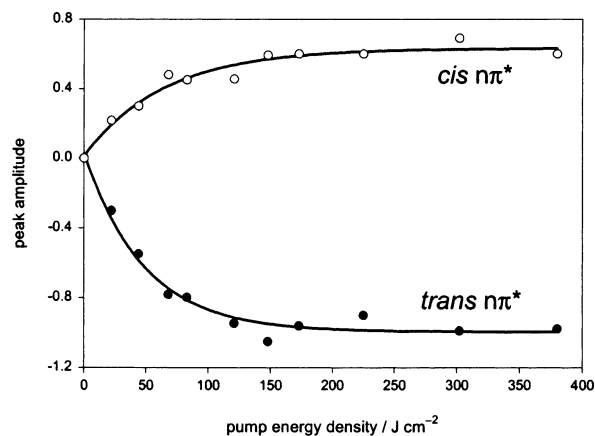


Figure 10. Results of the deconvolution of the dichroic spectra of Figure 8 into the two bands illustrated in Figure 9. The change in amplitude of the bands with increasing exposure is shown for peak centered at 470 nm by \bullet and the peak at 495 nm by \circ .

It is in general difficult to obtain information about the orientation of the cis isomers, but a recent dichroic infrared study by Buffeteau et al.⁶ has isolated individual $N=N$ stretching bands for trans and cis isomers of an unsubstituted amorphous azopolymer. The authors have found that the $N=N$ bond axis for both isomers is oriented parallel to the polarization direction of the pump but remark that the finding is different from typical results, at least for the trans isomer $N=N$ stretching observed for other azo polymers. A similar infrared study by Han et al.²⁸ was performed for the same polymer as in the current study, but at 76 °C for a 60 nm film. Although those authors have not made many band assignments in their spectrum, all of the bands

display clear negative dichroism, in agreement with our results for the amorphous film.

6.1. Proposed Mechanism To Account for the Positive Dichroism. To explain how this unusual orientation of the cis isomers arises for the annealed films, we propose the following mechanism. In the amorphous films the situation is straightforward: neither of the isomers can absorb the pump when their N=N axis is perpendicular to the polarization direction on account of the orientation of the transition moments. In the liquid crystalline films, the optical Fréedericksz transition (OFT) occurs as a result of the torque experienced by an induced dipole in the laser's electric field. The induced dipole will occur along the direction of highest polarizability. Although the cis isomers are bent, they are still more polarizable along the direction of the N=N bond axis than along a perpendicular molecular axis. By this reasoning, trans isomers should experience an even greater optical torque because they are even more polarizable due to their elongated shape. For the trans this force may not be relieved, however, because by the same token, they are too difficult to move in this manner on account of their greater structural anisotropy (rodlike shape). Cis isomers occupy more volume in the polymer matrix than trans, and as a consequence may be reoriented more easily by any mechanism. Although some of the cis isomers oriented in such a manner will be pumped into trans and thereby undergo reorientation, eventually to perpendicular (horizontal) states, the majority of the cis isomers will return to a vertical orientation by the OFT. Perhaps the self-aggregation characteristic of liquid crystals is responsible for stabilizing small domains of cis isomers.

The difference in the behavior between the two samples studied is a result of vastly different chromophore mobility. Before annealing, the polymer matrix is glassy at room temperature (50 °C below T_g) and cannot allow reorientation except by isomerization. After annealing, the polymer is considerably more fluid in its nematic liquid-crystalline phase, and therefore susceptible to the OFT.

We now account for the fact that such anomalous orientation/dichroism has not been reported by others working with the same or similar materials. Most reports of this material (including copolymers) have concentrated on thermal effects—amplification and destruction of anisotropy due to aggregation and randomization.^{28–31} There has also been recent interest in biaxiality observed as a consequence of in-plane and out-of-plane alignment during irradiation of this polymer.^{32–34} In all cases, orientation was reported as either in-plane with negative dichroism and/or birefringence or out-of-plane (parallel to the propagation direction in cases of an unpolarized pump). We have already mentioned that the material needs to be in its liquid-crystalline phase prior to irradiation to observe the anomalous cis alignment. There appears to be a second condition, however, which we have not studied in much detail: there is a threshold film thickness below which samples behave as amorphous films (no OFT), regardless of whether they have been annealed or not, and this is somewhere around 1 μm . Previous reports have used film thicknesses ranging from 50 to 150 nm. For thin films that have been annealed under the exact same conditions as described here, we observe a nematic Schlieren texture, just as in the thick films, but the domains are considerably smaller. Perhaps the mobility of the mesogens is sensitive to the local steric and/or electronic environment, which is somehow different with many nearby domain boundaries. Another possibility is that thinner films experience too much azimuthal surface anchoring from the glass substrate, thereby prohibiting reorientation by the OFT. The thinner films we prepared were

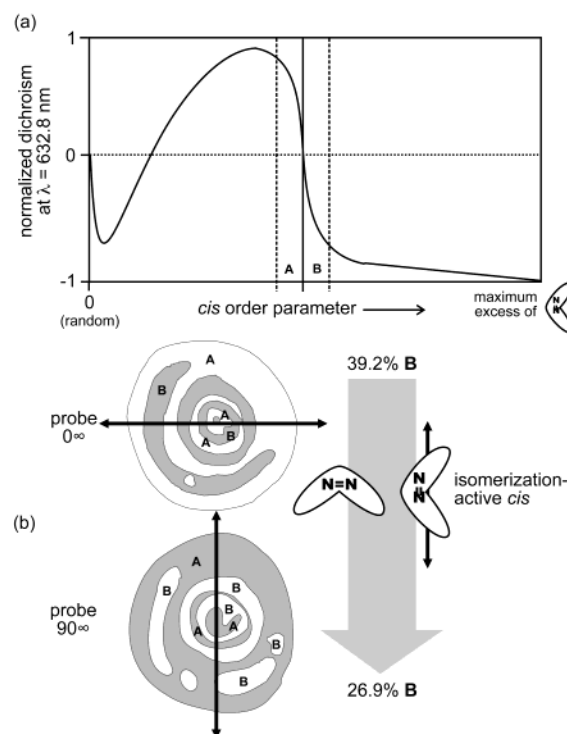


Figure 11. (a) Combining the information on the cis order parameter obtained from Figure 10 with the dichroism results from Figure 5a, a sketch of the dichroism vs order parameter profile may be constructed. (b) The first two dichroic micrographs from Figure 7 have been mapped according to the order parameter of the regions of opposing contrast. As the probe polarization is rotated, the order parameter decreases in favor of cis with their N=N axes perpendicular to the polarization direction.

difficult to characterize, as the results obtained for them were not reproducible, perhaps due to a subtle tradeoff between all of these factors. Demonstrations of OFT for other liquid crystals typically employ much thicker samples of 10–250 μm .^{15,18}

6.2. Proposed Mechanism To Account for the Quadrupolar Transmission Profile. Because oriented chromophores exist in liquid-crystalline domains, it is reasonable to assume that the order parameters suggested by the dichroic spectra in Figure 5a are not uniform over the entire irradiated area, and subdivisions of the probed area may show different directors or order parameters. In addition to the cis isomers with N=N axes parallel to the pump polarization, there is a smaller population of cis isomers with N=N axes perpendicular to the pump polarization, because they are trapped in such orientations in the trans–cis isomerization process. Combining the insight we have as to the order parameter of the cis based on the trends in Figure 10 with the corresponding dichroism observed at 632.8 nm from Figure 5a, we can make a sketch of dichroism vs order parameter, as shown in Figure 11. When the transmission profile appears symmetrically quadrupolar, as it does in Figure 6, plot 3 (transmittance is the same for 0°, 90°, 180°, and 270°), the dichroism averaged over the entire probed area should be zero, neglecting any dynamic movement of the domain walls. Domains with a local order parameter somewhere in region A of Figure 11a will appear bright when the polarizer is set to 0°. Domains with a slightly greater order parameter, somewhere in region B, will appear dark for the same polarizer orientation. The first two dichroic micrographs of Figure 7 are shown in Figure 11b with regions of opposite contrast labeled according to their order parameter. We observe that as the polarization of the probe light is varied from 0° to 90°, the relative total area

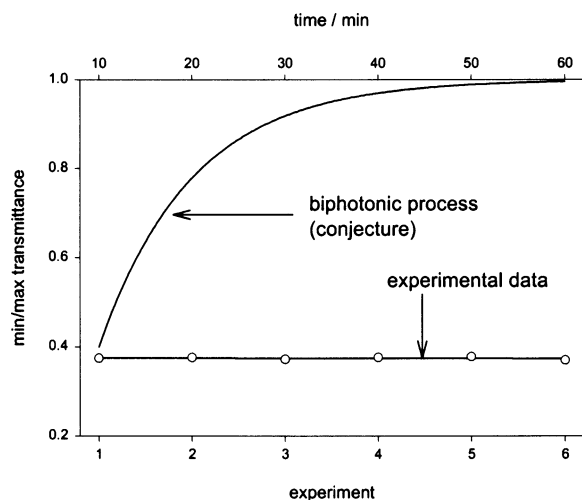


Figure 12. Ratio of the average minimum transmittance (obtained from measurements at 45°, 135°, 225°, and 315° counterclockwise from the positive x -axis) to the average maximum transmittance (taken from 0°, 90°, 180°, and 270°) obtained for six successive measurements. If this were a biphotonic process where the cis isomers are converted irreversibly to trans, this ratio would tend toward unity.

of regions A increases at the expense of regions B. From this we know that during the measurement, as the azimuth of the probe is changing, the order parameter decreases in favor of cis isomers with their N=N axes perpendicular to the probe polarization direction. This also points to an isomerization-based mechanism being responsible for the reorientation.

Because this is a photoinduced reorientation that likely involves isomerization, a biphotonic process would be a likely explanation. There have been many reports in the literature where long-lived cis are photochemically converted back to trans by illumination with red light such as that of our HeNe.^{35–41} Although such a biphotonic process may account for the general shape of the transmission profile, it alone cannot explain the reproducibility of the observed quadrupolar pattern. If the change in orientation were accompanied by a decrease in the cis population, the magnitude of the minimum-to-maximum transmittance would increase during one probing cycle as the probe's azimuth is varied through 360°. This ratio should approach unity (circular transmission profile) if not during one measurement, then at least after repeated measurements. Such an experiment is shown in Figure 12 where the ratio of the minimum-to-maximum transmittance is plotted for six consecutive measurements. During this time the sample has been exposed to the HeNe for about 1 h and there is no observable change in the magnitude of the intensity variation or absolute value of the transmittance for each azimuth. From this we conclude that whatever dynamic process is reorienting the chromophores, trans–cis as well as cis–trans isomerization must be occurring.

In a typical azo polymer, either amorphous or liquid crystalline, reorientation involving generation of cis from trans is not observed with red light because the absorption coefficient of trans in the red is vanishingly small. The consequence of this low probability of reaching the π^* excited state is that, even for a large number of photons, there will be very few transitions, and many trans–cis–trans cycles are required for reorientation. In our present situation, however, the existence of small highly ordered domains with various director distributions may allow a very small number of isomerization cycles to orient mesogens in the inter-domain (wall) regions. The mesogens that make up the domain walls experience a strong local field from ones in neighboring domains so only a small amount of energy is

required to effect their reorientation and apparent movement of the domain walls.

Such reorientation due to the HeNe may occur at any point in the Ar⁺ exposure, but it goes unnoticed when the area of the domains with larger order parameters is below a critical level, namely the level at which the dichroism in the red should be near zero. When the dichroism first changes sign (moving from region 1 into region 2 in Figure 5) no quadrupolar intensity distribution is seen, because the population of cis isomers with N=N axes parallel to the pump is not large enough to have a marked influence. In general, when the dichroism in the red is strongly positive (short exposures) or strongly negative (large exposures), a small perturbation in the orientation by the probe beam does not change the sign of the dichroism. For the smaller values of the dichroism observed in the second transition (between regions 3 and 4), a small perturbation in the order parameter may affect the sign of the observed dichroism, producing the quadrupolar transmission profile.

Finally, it is curious that the oriented domains that give rise to this transmission profile appear as concentric rings. The phenomenon of self-phase modulation occurs when a material, often a nematic liquid crystal, has a refractive index that depends on the laser intensity.⁴² The laser's Gaussian intensity profile then translates into a Gaussian index profile and, for thin films, a ringed diffraction pattern is observed in the far-field.^{22,43,44} It is possible that in these pMAB6 films, a radial modulation of the pump beam's intensity occurs as a result of varying phase shifts across the diameter of the irradiated area, and the order parameter observed in the dichroic maps picks up this intensity profile.

7. Conclusions

The polymer liquid crystal pMAB6 shows evidence of two electronic transitions in the lowest energy band of the dichroic UV–vis spectrum, assigned to the $n\pi^*$ bands of the trans and cis isomers. The convolution of the two dichroic bands, whose intensity depends on the order parameter, produces a dichroic spectrum that may be either positive or negative in the red. It is therefore necessary to be cautious in deducing orientation merely from the dichroism at a single wavelength.

For films that have not been annealed and are therefore in an amorphous state, our results suggest that the cis isomers are aligned with their N=N axes perpendicular to the polarization of the pump laser. This seems like it should be the normal behavior of this chromophore considering the angular dependent pumping that occurs in the isomerization-based photoorientation mechanism. In the case of films that are in a liquid crystalline phase and with sufficient thickness, our results suggest that the cis isomers are predominantly oriented with their N=N axes parallel to the pump polarization. We propose the optical Fréedericksz transition to be accountable for this alignment.

As another consequence of the occurrence of both OFT and concomitant orientation by isomerization, the generation of domains with a distribution of directors gives rise to a quadrupolar transmission profile for a certain range of exposures. This is attributed to a dynamic perturbation of the mesogen orientations by trans–cis–trans isomerization cycles.

Acknowledgment. We thank Dr. Yiliang Wu for the synthesis of pMAB6 and its phase characterization, and Ms. Lyn Kearns for the X-ray data. We thank the Natural Science and Engineering Research Council of Canada and the Department of National Defence (Canada) for funding this work. A.N.,

Canada Research Chair in Polymer Chemistry, is grateful to the CRC program of the Government of Canada. D.H. thanks the Government of Ontario for an OGS scholarship.

References and Notes

- (1) Rau, H. In *Photochemistry and Photophysics*; Rabek, J. F., Ed.; CRC Press: Boca Raton, FL, 1990; Vol. 2, p 119.
- (2) Monti, S.; Orlandi, G.; Palmieri, P. *Chem. Phys.* **1982**, *71*, 87.
- (3) Ishikawa, T.; Noro, T.; Shoda, T. *J. Chem. Phys.* **2001**, *115*, 7503.
- (4) Hirose, Y.; Yui, H.; Sawada, T. *J. Phys. Chem. A* **2002**, *106*, 3067.
- (5) Cattaneo, P.; Persico, M. *Phys. Chem. Chem. Phys.* **1999**, *1*, 4739.
- (6) Buffeteau, T.; Lagugné Labarthe, F.; Pézolet, M.; Sourisseau, C. *Macromolecules* **2001**, *34*, 7514.
- (7) Hochstrasser, R.; Lower, S. *J. Chem. Phys.* **1962**, *36*, 3505.
- (8) Harris, D.; Bertolucci, M. *Symmetry and Spectroscopy*; Dover: New York, 1978; pp 422–431.
- (9) Delaire, J.; Nakatani, K. *Chem. Rev.* **2000**, *100*, 1817.
- (10) Eich, M.; Wendorff, J. *Makromol. Chem., Rapid Commun.* **1987**, *8*, 59.
- (11) Rochon, P.; Gosselin, J.; Natansohn, A.; Xie, S. *Appl. Phys. Lett.* **1992**, *60*, 4.
- (12) Simoni, F.; Francescangeli, O. *J. Phys.: Condens. Mater.* **1999**, *11*, R439.
- (13) Ichimura, K. *Chem. Rev.* **2000**, *100*, 1847.
- (14) Fréedericksz, V.; Zolina, V. *Trans. Faraday Soc.* **1933**, *29*, 919.
- (15) Durbin, S.; Arakelian, S.; Shen, Y. *Phys. Rev. Lett.* **1981**, *47*, 1411.
- (16) Wong, G.; Shen, Y. *Phys. Rev. Lett.* **1973**, *30*, 895.
- (17) Hsiung, H.; Shi, L.; Shen, Y. *Phys. Rev. A* **1984**, *30*, 1453.
- (18) Ziyang, L.; Shi, J.; Ying, X.; Shi, L.; Jian, W.; Liang, Z.; Qiu, Z. *Phys. Lett. A* **2000**, *270*, 326.
- (19) Jánossy, I.; Lloyd, A. *Mol. Cryst. Liq. Cryst.* **1991**, *203*, 77.
- (20) Jánossy, I.; Szabados, L. *Phys. Rev. E* **1998**, *58*, 4598.
- (21) Jánossy, I. *Phys. Rev. E* **1994**, *49*, 2957.
- (22) Zhang, H.; Shiino, S.; Shishido, A.; Kanazawa, A.; Tsutsumi, O.; Shiono, T.; Ikeda, T. *Adv. Mater.* **2000**, *12*, 1336.
- (23) Angeloni, A.; Caretti, D.; Carlini, C.; Chiellini, E.; Galli, G.; Altomare, A.; Solaro, R. *Liq. Cryst.* **1989**, *4*, 513.
- (24) Hatada, K.; Kitayama, T.; Nishiura, T.; Tawada, M.; Harazono, T.; Sugaya, T. *J. Macromol. Sci.* **1997**, *A34*, 1183.
- (25) Hore, D.; Natansohn, A.; Rochon, P. *J. Phys. Chem. B* **2002**, *106*, 9004.
- (26) Todorov, T.; Nikolova, L.; Tomova, N. *Appl. Opt.* **1984**, *23*, 4309.
- (27) Natansohn, A.; Rochon, P.; Gosselin, J.; Xie, S. *Macromolecules* **1992**, *25*, 2268.
- (28) Han, M.; Morino, S.; Ichimura, K. *Macromolecules* **2000**, *33*, 6360.
- (29) Han, M.; Ichimura, K. *Macromolecules* **2001**, *34*, 90.
- (30) Meier, J.; Ruhmann, R.; Stumpe, J. *Macromolecules* **2000**, *33*, 843.
- (31) Han, M.; Ichimura, K. *Macromolecules* **2001**, *34*, 82.
- (32) Ichimura, K.; Han, M.; Morino, S. *Chem. Lett.* **1999**, 85.
- (33) Han, M.; Morino, S.; Ichimura, K. *Chem. Lett.* **1999**, 645.
- (34) Han, M.; Morino, S.; Ichimura, K. *Mater. Res. Soc. Symp. Proc.* **1999**, *559*, 159.
- (35) Ramanujam, P.; Hvilsted, S.; Andruzzi, F. *Appl. Phys. Lett.* **1993**, *62*, 1041.
- (36) Bach, H.; Anderle, K.; Fuhrmann, T.; Wendorff, J. *J. Phys. Chem.* **1996**, *100*, 4135.
- (37) Wu, P.; Wu, X.; Wang, L.; Xu, J.; Zou, B.; Gong, X.; Huang, W. *Appl. Phys. Lett.* **1998**, *72*, 418.
- (38) Wu, P.; Wang, L.; Xu, J.; Zou, B.; Gong, X.; Zhang, G.; Tang, G.; Chen, W. *Phys. Rev. B* **1998**, *57*, 3874.
- (39) Sánchez, C.; Alcalá, R.; Hvilsted, S.; Ramanujam, P. *Appl. Phys. Lett.* **2000**, *77*, 1440.
- (40) Sánchez, C.; Cases, R.; Alcalá, R.; López, A.; Quintanilla, M.; Oriol, L.; Millaruelo, M. *J. Appl. Phys.* **2001**, *89*, 5299.
- (41) Sánchez, C.; Alcalá, R.; Hvilsted, S.; Ramanujam, P. *Appl. Phys. Lett.* **2001**, *78*, 3944.
- (42) Khoo, I. *Optics and nonlinear optics of liquid crystals*; World Scientific: 1993.
- (43) Durbin, S.; Arakelian, S.; Shen, Y. *Opt. Lett.* **1981**, *6*, 411.
- (44) Khoo, I.; Hou, Y.; Liu, T.; Yan, P.; Michael, R.; Finn, G. *J. Opt. Soc. Am. B* **1987**, *4*, 886.